

Catalytic Degradation of Rhodamine B over FeMCM-41†

M. NOOKARAJU, A. RAJINI, N. VENKATATHRI and I. AJIT KUMAR REDDY*

Department of Chemistry, National Institute of Technology Warangal, Warangal-506 004, India

*Corresponding author: E-mail: iakreddy@nitw.ac.in

AJC-11766

Fe incorporated MCM-41 (FeMCM-41) is synthesized at room temperature by instant mixing of silica and iron precursors to a clear solution of surfactant following co-precipitation method. It is characterized by various physico-chemical techniques like PXRD, BET, FT-IR and SEM. The mesoporous character of the material has been established from BET adsorption desorption studies. Degradation of Rhodamine B in presence of hydrogen peroxide as oxidant over FeMCM-41 has been investigated. It is observed that 94.25 % of dye gets degraded in 150 min. It is found that degradation % increases with increase in pH and also with increase in the concentration of oxidant. Optimum conditions for the degradation of Rhodamine B by hydrogen peroxide over FeMCM-41 have been established.

Key Words: MCM-41, Functionalization, Dye degradation, Rhodamine B, Oxidation.

INTRODUCTION

Organic compounds present in wastewaters cause pollution to the aquatic environment. Among these, synthetic dyestuffs which are widely used in textile and printing industries cause serious environmental problems due to their presence in effluent waters^{1,2}. Rhodamine B is one of the most important and widely used xanthene dyes and is known for its high stability³. Thus, the treatment of effluents containing Rhodamine B is important for the protection of water and environment⁴. Dye removal from wastewaters by conventional methods like adsorption and flocculation is difficult owing to their low molecular weight and high water solubility⁵. These processes lead to the formation of sludge along with the dye content and cause disposal problems⁶. Recently photo-catalytic degradation of Rhodamine B was studied using titanium dioxide⁷⁻⁸, silver and indium oxide co-doped TiO₂⁹ and nano-sized zinc oxide powder¹⁰. Advanced oxidation processes (AOPs) like Fenton's process are also used as alternate methods for water treatment. Fenton's process is based on oxidation with Fenton reagent, which comprises an oxidative mixture of hydrogen peroxide and ferrous ions Fe²⁺ ion as catalyst¹¹. Major disadvantages of these methods are extensive use of harmful chemicals and reusability of the catalyst¹².

With a view to develop a simple and economical method for degradation of Rhodamine B, we have synthesized heterogeneous and reusable catalyst FeMCM-41 at room temperature by *in situ* incorporation of Fe in MCM-41 using co-precipitation

technique and characterized it. In this paper, we report our results on catalytic degradation of Rhodamine B by hydrogen peroxide in the presence of FeMCM-41. Effect of various reaction parameters like pH, oxidant concentration has been studied to establish optimum reaction conditions for efficient degradation.

EXPERIMENTAL

Tetraethyl orthosilicate was obtained from Sigma-Aldrich, cetyltrimethylammonium bromide was obtained from SD Fine Chemicals Ltd., India, ammonia (25%), ethyl alcohol and ferric nitrate were obtained from SRL laboratories, India. All the chemicals were of reagent grade and were used as obtained without further purification. Double distilled water was used throughout the reaction.

Synthesis of MCM-41 and FeMCM-41: Modified co-precipitation synthesis route¹³ was adopted for the preparation of FeMCM-41 under mild conditions in terms of temperature and surfactant quantity. 2.4 g of cetyltrimethylammonium bromide was dissolved in 120 mL of distilled water at room temperature and stirred continuously until a clear homogeneous solution was obtained. 10.2 mL of 25 wt. % aqueous ammonia was added to this homogeneous solution. 10 mL of tetraethyl orthosilicate was added drop by drop to the above mixture. The solution becomes milky and a gel is formed due to the hydrolysis of tetraethyl orthosilicate. To this gel 0.048 g of ferric nitrate was added to get Si/Fe ratio as 100 in the product. The gel was stirred further for about 2 h to

†Presented at International Conference on Global Trends in Pure and Applied Chemical Sciences, 3-4 March, 2012; Udaipur, India

get complete hydrolysis of tetraethyl orthosilicate. White precipitate thus formed was filtered and washed consecutively with distilled water and ethanol. This was dried at 110 °C overnight. Finally, the solid product was calcined at 550 °C in air atmosphere for 5 h in order to remove the surfactant. MCM-41 was prepared following the same method without addition of ferric nitrate.

Characterization of catalysts: The X-ray diffraction patterns were recorded in air atmosphere at room temperature on Philips X'Pert X-Ray diffractometer equipped with $\text{CuK}\alpha$ ($\lambda = 1.5406 \text{ \AA}$) radiation operating at 40 kV and 40 mA between 2θ angle range from 0.5 to 10° with a scan speed of $0.02^\circ \text{ s}^{-1}$. Nitrogen adsorption-desorption isotherms were measured using Quanta chrome surface area and particle size analyzer equipped with Novawin 2.0. All the samples were degassed at 200 °C for 4 h, prior to the N_2 adsorption-desorption analysis. The surface area of the materials was measured by using multi point BET model. The pore size distribution was obtained through the BJH model using desorption branch of the isotherm. Pore volume was estimated at a relative pressure of 0.99, assuming full surface saturation with nitrogen. The morphology of the synthesized MCM-41 and Fe incorporated MCM-41 was obtained from SEM images taken on Jeol electron microscope equipped with EDAX facility. The FTIR spectra were recorded 4000-450 cm^{-1} region using spectroscopic quality KBr powder with Jasco spectrometer.

Catalytic degradation of Rhodamine B: The degradation on Rhodamine B dye using hydrogen peroxide as oxidant in presence of FeMCM-41 has been studied at 25 °C. $1 \times 10^{-3} \text{ M}$ stock solution of Rhodamine B was prepared and experimental solutions of desired concentration have been obtained by the successive dilutions of the stock solution. The degradation studies have been followed by using a UV-Visible spectrophotometer by measuring decrease in the absorbance of the solution at 550 nm with respect to time. The effect of varying pH, concentration of Rhodamine B and concentration of hydrogen peroxide on the degradation of the dye has been studied. The % of degradation of the dye has been calculated by using the formula

$$\% \text{ degradation} = (A_0 - A_t) / A_0 \times 100.$$

where A_0 = Absorbance at initial time and A_t = Absorbance at time t .

RESULTS AND DISCUSSION

XRD patterns of MCM-41 and also metal incorporated MCM-41 samples show only one low angle peak at 2θ value of 2.2° corresponding to the meso phase¹⁴, which is the characteristic of the long range hexagonal structure of MCM-41. This low value of 2θ is mainly due to the length of the carbon chain used for synthesis of MCM-41. With the incorporation of Fe^{3+} ion into the frame work of mesoporous materials, the intensity of low angle peak decreased. This indicates the occupancy of metal ion in the place of Si. The surface Si ions were replaced isomorphously by the guest iron ions. It was also observed that there is no appreciable change in the peak position in the XRD patterns of MCM-41 and FeMCM-41. This reveals that the lattice structure of metal incorporated MCM-41 remains mesoporous and is similar to that of parent

MCM-41 material. The X-ray diffraction pattern for MCM-41 and FeMCM-41 is shown in Fig. 1.

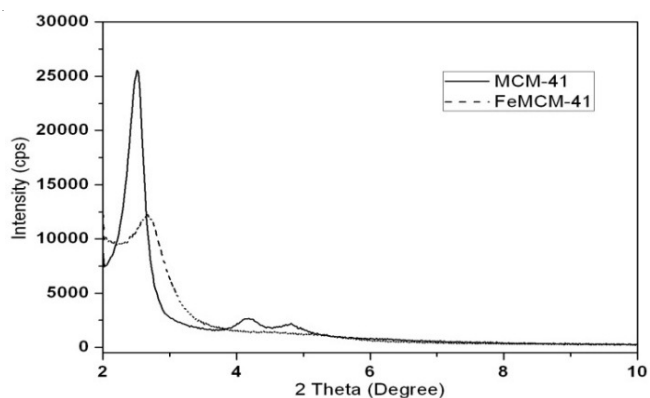


Fig. 1. X-ray diffraction pattern for A) MCM-41 and B) FeMCM-41

The nitrogen adsorption-desorption isotherms of MCM-41 and FeMCM-41 of the materials are shown in Fig. 2. The surface areas of the synthesized MCM-41 and Fe incorporated MCM-41 materials were found to be $1032 \text{ m}^2\text{g}^{-1}$ and $793.9 \text{ m}^2\text{g}^{-1}$ respectively.

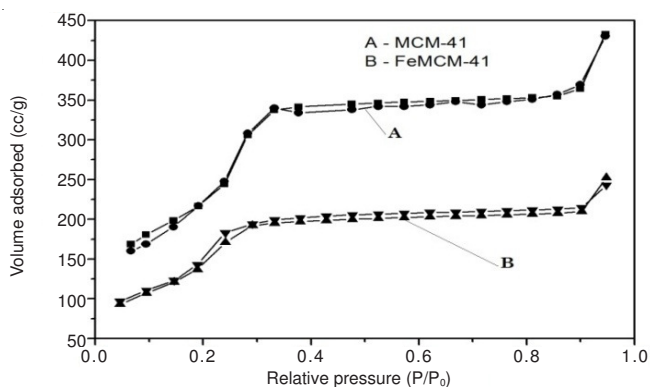


Fig. 2. Nitrogen Adsorption-Desorption isotherms for A) MCM-41 and B) FeMCM-41

Fig. 2 showed that both the adsorption isotherms follow the typical type-IV adsorption isotherm patterns indicating the mesoporous character of the materials¹⁵. The pore volume and pore radius of the materials were found to be in nano scale.

FTIR spectra of MCM-41 and FeMCM-41 are shown in Fig. 3. In the hydroxyl region ($3600\text{--}3200 \text{ cm}^{-1}$), a broad band is seen around 3408 cm^{-1} , which is attributed to surface silanols and adsorbed water molecules. The absorption bands close to 1630.5 cm^{-1} is due to the bending vibration of adsorbed water molecules. The asymmetric stretching vibrations of Si-O-Si are observed by the absorption bands at 1088 and 1235 cm^{-1} ¹⁶. The band at 962 cm^{-1} can be attributed to Si-OH vibrations. The absorption peaks around 450 to 795 cm^{-1} can be assigned to bending vibration of Si-O-Si bond. The band at 802 cm^{-1} corresponds to free silica. The FTIR spectra of FeMCM-41 closely resemble that of Fe free MCM-41 and a band at 960 cm^{-1} is clearly visible. The strong intensity of this band in pure MCM-41 is due to the large amount of silanol groups present in the material¹⁷. The decrease in the intensity of this band in FeMCM-41 indicates the surface modification of MCM-41.

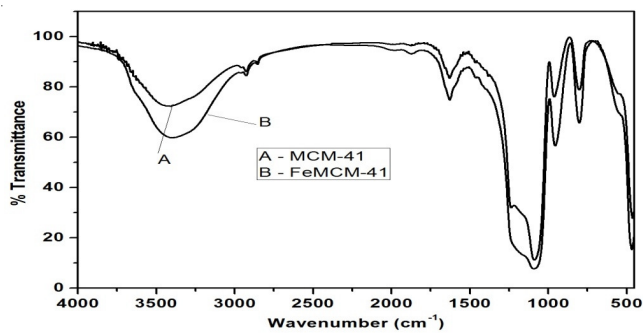


Fig. 3. FTIR Spectra of A) MCM-41 and B) FeMCM-41

The SEM images of MCM-41 and FeMCM-41 materials are shown in Fig. 4. It can be observed that the morphology of the material is spherical and remains same even after the surface modification with Iron¹⁸. From EDAX studies, the presence of Fe ion on the surface and in bulk of the MCM-41 framework is confirmed. From EDAX spectrum, the % loading of iron in the frame work has been found to be 60.46 % with respect to Si.

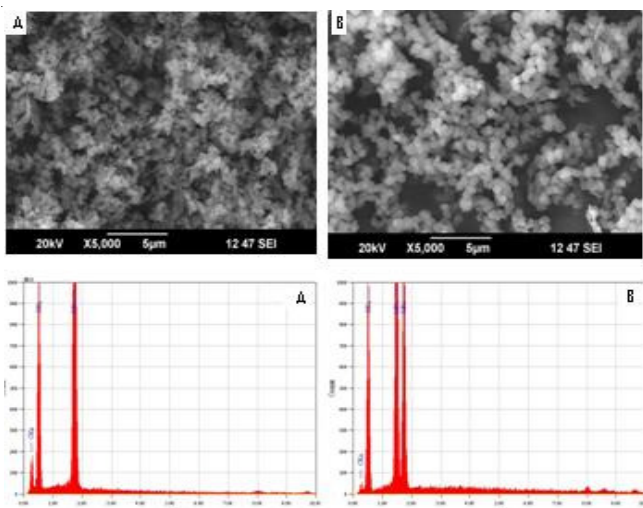


Fig. 4: SEM-EDAX images of A) MCM-41 and B) FeMCM-41

Catalytic degradation of Rhodamine B over FeMCM-41

Effect of hydrogen peroxide concentration: Effect of varying concentration of oxidant on degradation of Rhodamine B has been investigated at room temperature in the range of 2.3×10^{-3} M to 7.2×10^{-3} M of hydrogen peroxide. The degradation of Rhodamine B increased with increase in concentration of hydrogen peroxide till 5.8×10^{-3} M and it is found to be decrease slightly at 7.2×10^{-3} M. This decrease in the % degradation at higher hydrogen peroxide concentration can be attributed to the formation of OH⁻ ions rather than OH[•] radicals which interact with Fe³⁺ ions in the matrix of MCM-41 thereby hindering the rate of degradation. Degradation reaction of Rhodamine B with hydrogen peroxide takes place due to the attack of hydrogen peroxide on the C-C bond in the central ring structure of Rhodamine B. The % of degradation of Rhodamine B is found to be 94.25 % in 150 min of reaction (Fig. 5 and Table-1).

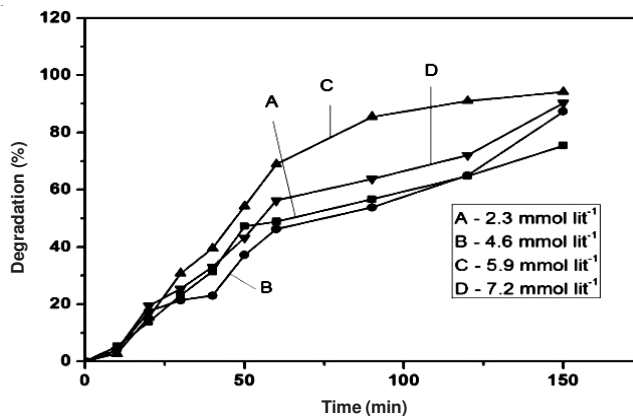


Fig. 5. Effect of hydrogen peroxide on degradation of Rhodamine B

Hydrogen peroxide [M]	Degradation (%)
2.3×10^{-3}	75.47
4.6×10^{-3}	87.34
5.8×10^{-3}	94.25
7.2×10^{-3}	90.34

Effect of pH: Effect of pH on degradation of Rhodamine B has been investigated at room temperature in the pH range of 2-10. The degradation of Rhodamine B by hydrogen peroxide over FeMCM-41 was found to be increase with increase in pH till the solution is slightly basic and in strong alkaline conditions, the extent of degradation decreased slightly¹⁹. Small decrease in the extent of degradation at higher pH can be attributed to the formation agglomerates of hydroxides (Fig. 6 and Table-2).

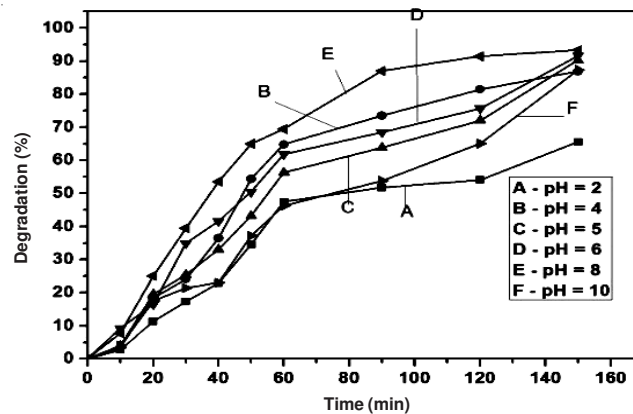


Fig. 6. Effect of pH on degradation of Rhodamine B

pH	Degradation (%)
2	65.57
4	86.9
5	90.34
6	91.57
8	93.32
10	87.34

Effect of Rhodamine B concentration: Degradation of Rhodamine B was carried out at 25 °C in the presence of

hydrogen peroxide at varying concentrations of Rhodamine B in the range of 1×10^{-4} M to 7×10^{-4} M. The % of degradation is found to increase with increase in concentration of Rhodamine B. With the increase in concentration of Rhodamine B the amount of hydrogen peroxide required for the degradation is found to increase which leads to the limit for the concentration of Rhodamine B²⁰. The degradation of Rhodamine B in a concentration range of 1×10^{-4} M to 5×10^{-4} M of Rhodamine B has been found to increase and there is no much change in % degradation with further increase in concentration of Rhodamine B (Fig. 7 and Table-3).

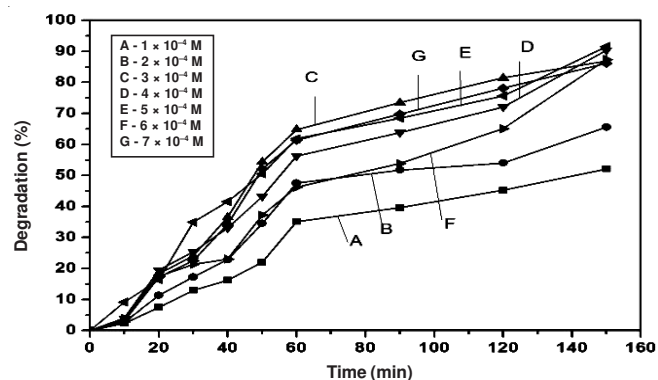


Fig. 7. Effect of concentration of Rhodamine-B on degradation of Rhodamine B

TABLE-3
EFFECT OF RHODAMINE B ON % DEGRADATION
OF RHODAMINE B

Rhodamine B [M]	Degradation (%)
1×10^{-4}	52.12
2×10^{-4}	65.57
3×10^{-4}	86.9
4×10^{-4}	90.34
5×10^{-4}	91.57
6×10^{-4}	87.34
7×10^{-4}	86.12

Reusability: The possibility of reusing the catalyst was examined to see the cost effectiveness of the method. It was observed that the used catalyst could be used for the second time with 90 % efficiency. The regeneration of the catalyst could be done in a simple way. After the degradation of the dye the solution was kept standing for 12 h and then the supernatant liquid was decanted to separate catalyst. The catalyst is then thoroughly washed with distilled water and reused for the degradation of dye with a fresh dye solution.

Catalyst reusability	Cycle 1	Cycle 2	Cycle 3
Degradation (%)	94.25	90.15	89.2

Conclusion

MCM-41 and FeMCM-41 were synthesized by room temperature co-precipitation method. The materials were characterized for their morphological properties by PXRD, BET, SEM and FTIR techniques. The XRD patterns show the hexagonal arrangement of pores, BET adsorption isotherms reveal the mesoporous character of the material. SEM images confirm the spherical morphology of the material. Catalytic effect of FeMCM-41 towards the degradation of Rhodamine B revealed that 94.25 % of dye gets degraded in 150 min. The optimum conditions for the degradation of 5×10^{-4} M Rhodamine B have been found to be 5.8×10^{-3} M of hydrogen peroxide and pH-8. The catalyst has been tested for its reusability by carrying out the reaction over three cycles and it is found that the % of degradation remains nearly same in subsequent cycles.

REFERENCES

- M. Inoue, F. Okada, A. Sakurai and M. Sakakibara, *Ultrason. Sonochem.*, **13**, 313 (2006).
- T. An, H. Gu, Y. Xiong, W. Chen, X. Zhu, G. Sheng and J. Fu, *J. Chem. Technol. Biotechnol.*, **78**, 1142 (2003).
- P.C. Fung, Q. Huang, S.M. Tsui and C.S. Poon, *Water Sci. Technol.*, **40**, 153 (1999).
- G. Ruppert, R. Bauer and G. Heisler, *Chemosphere*, **28**, 1447 (1994).
- N. Azbar, T. Yonar and K. Kestioglu, *Chemosphere*, **55**, 35 (2004).
- C. Chen, P. Lei, H. Ji, W. Ma, J. Zhao, H. Hidaka and N. Serpone, *Environ. Sci. Technol.*, **38**, 329 (2004).
- J. Li, L. Li, L. Zheng, Y. Xian and L. Jin, *Electrochim. Acta*, **51**, 4942 (2006).
- M.A. Behnajady, N. Modirshahla, S.B. Tabrizi and S. Molanee, *J. Hazard. Mater.*, **152**, 381 (2008).
- X. Yang, L. Xu, X. Yu and Y. Guo, *Catal. Commun.*, **9**, 1224 (2008).
- H. Kisch and W. Macyk, *Chem. Phys. Chem.*, **3**, 399 (2002).
- N. Barka, S. Qourzal, A. Assabbane, A. Nounah and Y.A. Ichou, *J. Photochem. Photobiol. A: Chem.*, **195**, 346 (2008).
- D. Yu, R. Cai and Z. Liu, *Spectrochim. Acta A*, **60**, 1617 (2004).
- M. Grun, K.K. Unger, A. Mastumoto and K. Tsutsumi, *Micropor. Mesopor. Mat.*, **27**, 207 (1999).
- A. Corma, *Chem. Rev.*, **97**, 2373 (1997).
- M.T. Anderson, J.E. Martin, J.G. Odinek and P.P. Neeconer, *Chem. Mater.*, **10**, 311 (1998).
- G. Petrini, A. Cesana, G. De Alberti, F. Geroni, G. Leofanti, M. Padovan, G. Paparatto and P. Rofia, *Stud. Surf. Sci. Catal.*, **68**, 761 (1991).
- T. Blasco, A. Corma, M.T. Navarro and J.P. Pariente, *J. Catal.*, **156**, 65 (1995).
- A. Zecchina, G. Spoto, S. Bordiga, A. Ferrero, G. Petrini, G. Leofanti and M. Padovan, *Stud. Surf. Sci. Catal.*, **69**, 251 (1991).
- M.Y. Ghaly, G. Hartel, R. Mayer and R. Haseneder, *Waste Manage.*, **21**, 41 (2001).
- X. Xu, W. Zhao, Y. Huang and D. Wang, *J. Environ. Sci.*, **15**, 475 (2003).